Experimental characterization and performance benchmarking of magneto-rheological fluids for automotive brakes

Materials Research Express

PAPER

OPEN ACCESS

RECEIVED
19 January 2026

REVISED
3 June 2026

ACCEPTED FOR PUBLICATION
12 June 2026

PUBLISHED
24 June 2026

Experimental characterization and performance benchmarking of magneto-rheological fluids for automotive brakes

Giovanni Imberti[1], **Henrique de Carvalho Pinheiro**[1,*], **Massimiliana Carello**[1], **Lucia Tsantilis**[2] **and Rajandrea Sethi**[2]

[1] Department of Mechanical and Aerospace Engineering DIMEAS, Politecnico di Torino, Torino 10129, Italy
[2] Department of Environment, Land and Infrastructure Engineering DIATI, Politecnico di Torino, Torino 10129, Italy
[*] Author to whom any correspondence should be addressed.

E-mail: henrique.decarvalho@polito.it

Keywords: magneto-rheological fluid, automotive brake, rheology, sedimentation, performance benchmarking, smart materials

Abstract

Magneto-rheological (MR) fluids are smart materials that can change from liquid to semi-solid when exposed to a magnetic field. This property is useful for creating advanced devices like brakes and clutches. This paper addresses a gap in research by comparing different benchmarking methods for MR fluids. We analyse five commercially available MR fluids to identify key performance indicators for automotive braking applications. The study involves rheological tests to measure flow characteristics, scanning electron microscopy to analyse particle structure, and sedimentation tests to evaluate long-term stability. By correlating the fundamental properties of these fluids with the demands of braking applications, this work aims to establish a standardized framework for selecting the optimal MR fluid for a specific use case. This framework provides reliable data that can be integrated into simulation environments for virtual testing and validation.

1. Introduction

Magneto-rheological (MR) fluids represent a prominent class of 'smart' or 'field-responsive' materials, engineered materials whose properties can be rapidly and reversibly controlled by an external stimulus [1]. The fundamental composition of an MR fluid involves a suspension of micron-sized, magnetically particles, such as iron, within a non-magnetic carrier liquid like oil. The defining characteristic of these fluids, which underpins their technological significance, is their ability to undergo a significant phase transition. In the absence of a magnetic field (the 'off-state'), an MR fluid behaves as a conventional, free-flowing liquid. However, upon the application of an external magnetic field (the 'on-state'), it transforms into a semi-solid, viscoelastic material in a matter of milliseconds. This transformation is the physical manifestation of the suspended particles polarizing and aligning into chain-like, fibrous structures parallel to the magnetic flux lines. These structures create an internal framework that resists shear and flow, giving the fluid a controllable yield stress. It is this controllable, field-dependent yield stress that enables the design of advanced electromechanical devices, including high-performance brakes, clutches, and dampers.

The Innovative electric and hybrid vehicle research group developed ZEDS—zero-emissions driving system—a novel driving solution completely zero-emissions, combining an electric motor with a MR brake [2]. The solution has been developed and tested through a preliminary virtual validation [3] and then assessed during a complete testing procedure [4], fitting the braking targets requested for an automotive application. The final scope of the ZEDS solution is to integrate a novel and completely zero-emissions braking system to reducing harmful and critical pollutants generated by the actual disk-braking system [5]. A close examination of the body of research on MR fluids reveals a functional dichotomy between two primary communities. On one hand, materials scientists and chemists focus on the fundamental aspects of fluid formulation, dedicating their efforts to optimizing particle synthesis, discovering novel carrier fluids, and developing sophisticated additive packages to enhance properties like yield stress and sedimentation stability [6–8], while on the other hand, mechanical and systems

engineers concentrate on device design, integration, and control, applying MR fluids to create brakes, dampers, and clutches [9–11].

This paper seeks to address this critical gap by systematically collating and analysing the disparate benchmarking methodologies reported in the literature. The objectives of this report are:

- To critically analyse the rheometric and device-level testing procedures employed for their characterization
- To identify and consolidate the key performance indicators (KPIs) that serve as the basis for benchmarking; and fourth, to correlate these fundamental properties with the specific performance demands of end-applications, with a particular focus on MR brakes.

By synthesizing this information, this paper aims to provide a coherent framework to guide future research and development, to identify and select the optimal magnetorheological fluid (MRF) according to the expected application outcome, following a consistent and reliable testing procedure, concluding, as an output, with data suitable to be used into a simulation environment.

2. Method

The paper describes the scientific activities divided into three sections:

- Testing procedures
- Experimental results analysis
- Fluid-dynamic curves extrapolation for virtual correlation

The first part is the comparative analysis between 5 MRFs selected as benchmarking from different suppliers which specific fluid name has been reported in table 1. From this point on, the fluids will be mentioned with the described nomenclature of table 1 in order to make easier for the reader to go through the discussion.

Such fluids present standard data relied in the official datasheets and reported in table 2

Fluids performances have been tested into a rheometer for evaluating their rheological characteristics for extrapolating the yield curves, their particles have been analysed into the scanning electron microscopy (SEM) for microscopically understanding their differences and a sample for each fluid has been checked for a sedimentation analysis. These three procedures allow to have a complete breakdown of each fluid.

2.1. Sample preparation

Prior to each measurement, the MRF was re-homogenized to counteract particle sedimentation and ensure sample consistency. This was accomplished by subjecting the fluid to mechanical agitation for a period of 5–10 min with a standard laboratory mixer. A low rotational speed of 1400 rpm was deliberately chosen for this process to mitigate two potential issues: the generation of localized heat that could alter the fluid's properties, and mechanical degradation of the suspended particles by the mixer's impeller.

The adequacy of the homogenization was confirmed through a visual inspection of the container, verifying the absence of any discernible sediment at the bottom. This step is critical, as minor fluctuations in particle concentration can substantially affect the rheological characteristics of the fluid, potentially invalidating the results.

For precise volume dispensing and to enhance experimental repeatability, a calibrated variable-volume micropipette (100–1000 μl) was utilized. Due to the adhesive nature of the MRF's carrier oil, a reverse pipetting technique was employed to ensure accurate and consistent sample delivery. This method involves depressing the plunger completely to aspirate the fluid, then dispensing the required volume by returning the plunger to the first stop. By doing so, a small amount of liquid remains in the disposable tip, which acts as a liquid piston to expel the target volume and overcome adhesion forces. This approach successfully limited the volumetric variation between dispenzations to a negligible 3–5 μl, thereby ensuring the integrity and reliability of the subsequent analyses.

Table 1. List of magneto-rheological fluids under test.

Fluid type	Reference name
CK-MATERIAL MCR-C1R	MRF 1
FRAUNHOFER CUSTOM	MRF 2
LORD MRF132DG	MRF 3
LIQUID RESEARCH MRHCCS4-B	MRF 4
SOMAGNAR MS-R	MRF 5

Table 2. Baseline data from MRF benchmark datasheets.

Fluid Type	Viscosity (Pa-s @40 °C)	Density (g Cm^{-1}^3)	Solid continent (%)
MRF 1	0.079	2.7–3.0	—
MRF 2	—	—	88.0
MRF 3	0.112	2.95–3.15	80.98
MRF 4	—	3.45	85.0
MRF 5	0.35	3.4	81.0
Fluid type	**Flash point (°C)**	**T range (°C)**	**MAX Yield stress (kPa)**
MRF 1	—	−40 to 140	70 @ 450 kA m^{-1}
MRF 2	>180	−40 to 170	140 @ 640 kA m^{-1}
MRF 3	>150	−40 to 130	48 @ 290 kA m^{-1}
MRF 4	>160	−40 to 140	67 @ 740 kA m^{-1}
MRF 5	—	−40 to 175	100 @ 640 kA m^{-1}

2.2. Experimental setup

2.2.1. Rheological tests

The different rheological properties of the MRF were studied with an Anton Paar MCR 301, Graz, Austria in different measurement configurations. For the characterization under application of magnetic field, in order to evaluate both on- and off-state conditions, the rheometer was equipped with an MRD-70/1 T magnetocell (Anton Paar) equipped with a parallel-plate (PP) spindle geometry. The validation of the measuring geometry as well as the homogeneity of the field generated is well established by many authors [12]. The cell allows the generation of a homogeneous field up to 1 T in the region between the measuring plates, facilitated by an upper yoke that efficiently closes the magnetic circuit in close proximity to the plate.

The shear rate range is limited to 1000 s^{-1}.

Temperature control is achieved by a thermocirculator, namely the LAUDA Ecoline RE 207 (Königshofen, Germany), which allows regulation across a wide range of temperatures (−30 °C to 90 °C). For the tests, however, since the magnetocell has an upper limit of 70 °C, a working temperature ranges from 10 °C to 65 °C was selected.

2.2.2. Sedimentation test

To evaluate the long-term colloidal stability of each fluid formulation, a static sedimentation test was conducted. Following the standard homogenization procedure, a 14 ml aliquot of each fluid was decanted into a separate 15 ml graduated tube. The samples were subsequently stored in an undisturbed state at ambient laboratory conditions and monitored over a 200 d period. The volume of the clear supernatant oil that separated at the fluid's free surface was periodically recorded. These measurements were then used to calculate the sedimentation ratio for each sample, expressed as the volume percentage of separated oil relative to the total initial volume.

2.2.3. SEM analysis

The morphology and elemental composition of the metallic particles were investigated using SEM Leo Supra [13]. To prepare the samples, the particles were first isolated from the base oil through a solvent extraction technique. This process, conducted under a fume hiood involved mixing the MRF with cyclohexane, a solvent in which the oil is miscible. The mixture was agitated, and the metallic particles were allowed to sediment. A small magnet was used externally to hold the ferromagnetic particles at the bottom of the beaker during decantation of the oil-solvent mixture, thereby minimizing sample loss. This washing procedure was repeated 3–5 times to ensure all organic residue was removed, after

which the purified powder was dried by evaporating the remaining solvent. The cleaned particles were then mounted on aluminium stubs that had been cleaned with isopropyl alcohol and affixed with conductive carbon tape. A small quantity of the powder was applied to the tape using a spatula, and any excess was removed to prevent particle stratification and ensure high-quality imaging. The prepared stub was loaded into the SEM analysis chamber, which was subsequently evacuated to achieve an ultra-high vacuum. For analysis, the electron beam was activated and calibrated by setting the working distance to 6–8 mm, followed by focusing, beam centring, and astigmatism correction at magnifications exceeding 10000×. High-resolution micrographs were then acquired at resolutions of up to 8k to thoroughly characterize the particle structure.

After the characterization, the pictures have been analysed for extrapolating the average particle dimensions distribution in each fluid, in order to obtain a microscopical definition of each material to extract data useful for the rheological comparison as described by [14].

2.3. Significant parameters for the final application

The experimental tests were designed to quantify specific KPIs that directly correlate with the performance of an automotive braking system.

- Off-state flow curve: These measurements are critical for evaluating the parasitic drag or rolling resistance generated by the braking system when it is not engaged (e.g. while the vehicle is cruising). Lower shear stress at a given shear rate is desirable for maximizing vehicle efficiency.
- On-state flow curve: These measurements define the fluid's behavior at maximum magnetization and are used to determine the total available braking torque. Higher shear stress is essential for achieving high-performance braking, particularly in emergency situations.
- Static yield stress: Determined via a controlled shear stress test, this KPI represents the torque required to initiate viscous flow from a static condition. It corresponds to the 'holding' or 'breakaway' torque of the brake, which is important for applications like hill-hold assist.
- Magneto-sweep curve: This test characterizes the fluid's direct response to the applied magnetic field. The resulting curve is pivotal for developing control strategies and for assessing the fluid's energy efficiency—that is, its ability to generate high shear stress with a minimal applied magnetic field and, consequently, lower electrical current.
- Sedimentation stability: This KPI is fundamentally important for long-term reliability. Any significant phase separation in an automotive application could severely impair braking performance and compromise vehicle safety.

The testing procedures for these characterizations were iterated for each fluid following the detailed protocol described by Peruzzi *et al* [15], ensuring consistency across all measurements.

2.4. Testing procedures

The procedure followed has been described by Peruzzi *et al* [15], and the samples for each fluid consist of a volume of 0.4 ml tested in a PP setup with a gap of 1 mm. Following the reference methodology, this specific gap size is critical for evaluating the shear stress versus magnetic flux relationship: reducing the gap below 1 mm leads to excessive rolling resistance, which hinders the system's overall efficiency. On the other hand, at gaps above 1 mm, it was found to be impossible to perform any analysis due to the lack of proper contact between the fluid and the rotating plate. Therefore, the 1 mm gap ensures an optimal balance between creating strong magnetic structures for adequate torque and maintaining a manageable rolling resistance for smoother operation.

The rheological properties of the MRF were systematically characterized through three distinct experimental protocols to evaluate its dependence on temperature, magnetic field intensity, and shear rate. Firstly, dynamic flow curve measurements were performed in both off-state (0 T) and on-state (up to 0.9 T) conditions using a shear-rate-controlled protocol. After a pre-shear step at 20 s^{-1} to negate any shear history, the fluid was subjected to a logarithmic shear rate ramp from 1 s^{-1}–1000 s^{-1} under isothermal conditions ranging from 10 °C to 90 °C. For on-state tests, the magnetic field was applied for 30 s prior to the shear ramp to ensure the complete formation of field-induced particle structures. Secondly, the static yield stress was determined via a controlled shear stress test, where a logarithmic stress ramp from 1 kPa to 50 kPa was applied to the sample at rest, with the yield point identified by the onset of rapid viscous flow.

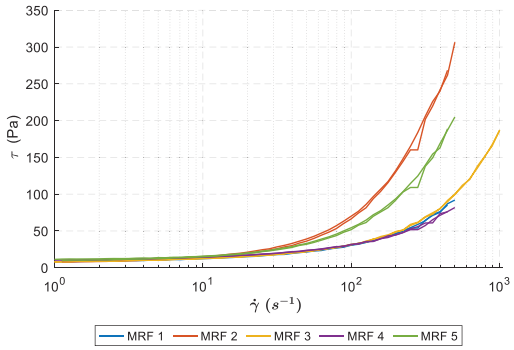

Figure 1. Rheological fluid comparison—shear stress vs shear rate at zero magnetic field.

It is important to note that for all data acquired using the PP geometry, a standard correction was applied to convert the measured apparent shear stress (τ_{aR}) to the true shear stress (τ_R), accounting for the fluid's non-Newtonian nature as reported in equation (1).

$$\tau_{a_R} = \frac{2M}{\pi R^3} \text{Where} \tau_R = \tau_{a_R}\left(\frac{3+n'}{4}\right); n' = \frac{\mathrm{d}\,(\log M)}{\mathrm{d}\,(\log \gamma_R)} \tag{1}$$

where T represents the measured torque and is the true rim shear rate. From our experimental data, the correction factor consistently ranged between 0.7 and 0.8, leading to an average overestimation of the shear stress by approximately 25%. This indicates that analyses based on apparent parameters without correction are significantly flawed and yield inaccurate results [16].

This correction was significant, as uncorrected data led to an average overestimation of shear stress values by approximately 25%, underscoring the necessity of this data processing step for accurate characterization.

3. Results

Describing the test results one after the other reporting the graphs and describing the procedure for each one.

3.1. Rheological characterization

The rheological characterization has been performed extracting data from the tests:

- Flow curve measurements in off-state conditions
- Flow curve measurements in the on-state conditions
- Controlled shear stress test
- The magneto-sweep method

The procedure followed has been described by Peruzzi *et al*[15] and the samples for each fluid is of a volume of 0.4 ml tested in a PP setup with a gap of 1 mm. The temperature is kept constant at 25 °C.

For the temperature it has been chosen to replicate the benchmarking characterization as a standard environmental temperature, although, once a fluid has been chosen for a specific application is important to complete the whole thermal characterization suggested by [15].

In figure 1 it is possible to see the results of the different shear stresses of the fluid at the variation of the shear rate during the off-state. It is possible to see how the variation, as expected is growing exponentially as a function of the speed. At slower shear rates, all the fluids have a similar behaviour, while, with the shear rate increasing, MRF 2 and MRF 5 are the two reaching the higher values.

The impact of MRF2 and MRF5 is also evident looking at figure 2, where MRF 2 has significantly higher values of shear stress respect the other fluids while the constant magnetization is equal to 0.85 T. This result means that MRF2 has the higher peak shear stress available at maximum magnetization, fitting it for the high torque request applications. It is also important to notice in figure 2 as the shear stresses are not anymore increasing exponentially, as the prime feature of the MRF is to generate a constant shear through different speeds due to the magnetization, behaving like a semi-solid.

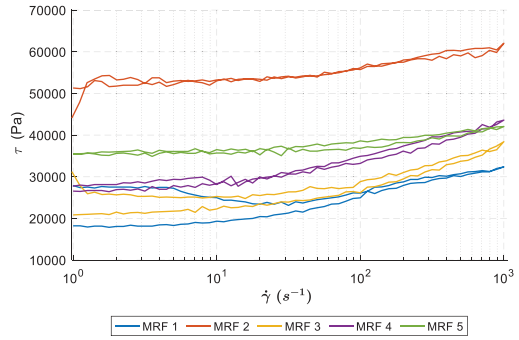

Figure 2. Rheological fluid comparison—shear stress vs shear rate at 0.85 T magnetic field.

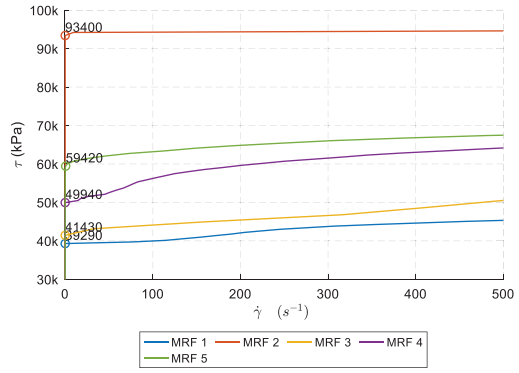

Figure 3. Rheological fluid comparison—controlled shear stress test at growing shear rate.

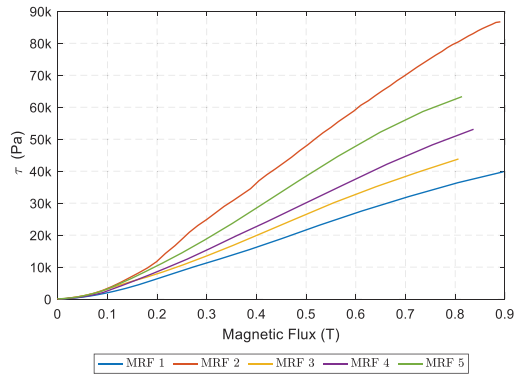

Figure 4. Rheological fluid comparison—magneto-sweep.

The major shear stress of the MRF2 is also visible in figure 3, where the magnetic field is kept constant at 0.85 T for obtaining the results of the controlled shear stress test increasing the shear rate. The results describe the points where each fluid comes from a solid-state behaviour to a liquid-phase ones, allowing to understand the peak braking performance the fluid could give into the automotive braking application.

The analysis of the magneto-sweep shown in figure 4, allows to evaluate the magnetic response of each fluid, showing the variation of the shear stress as a function of the magnetic flux applied.

It is possible to underline how, although all the curves are different one to another, they follow the same trend proportional to the peak value of shear stress already shown in figure 2, meaning that the magnetic response of the different fluid is quite similar and the metal particles have similar magnetic properties.

In order to compare the obtained results with the datasheet presented, in table 3 the list of yield stresses has been reported at 0.8 T.

Table 3. Max yield stress reached at 0.8 T.

Fluid type	MAX yield stress (kPa)
MRF 1	35
MRF 2	80
MRF 3	44
MRF 4	50
MRF 5	63

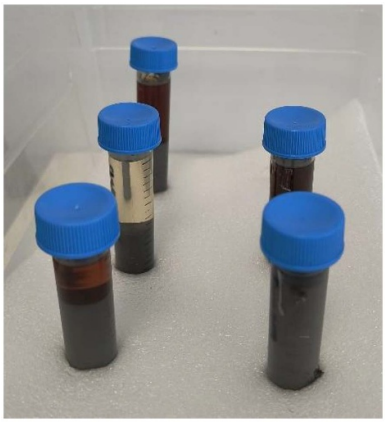

Figure 5. Sedimentation test—samples after the test.

3.2. Sedimentation analysis

The development of stable MR fluids is critically dependent on the ability to accurately and reliably quantify their sedimentation behaviour. Over the years, a diverse array of characterization techniques has been employed, ranging from simple visual methods to sophisticated, automated systems. Each method possesses distinct advantages and limitations, and the choice of technique often represents a trade-off between detail, practicality, and relevance to a specific application. A significant challenge in the field is the lack of a unified, standard method for evaluating stability, which complicates the direct comparison of results across different studies [17].

Although there are multiple complex sedimentation analysis strategies, considering multiple operative conditions, from centrifugal separation test [18] to magnetic flux density sensing [19], it has been decided to follow a simpler visualization method, helpful for understanding the free surface separation between the pure oil and the metal particle mixture [7], the most straightforward and widely used method.

This method relies on the direct, optical observation of the phase separation that occurs as particles settle in a transparent container, after being mixed.

The height of the clear supernatant liquid (H_s) that forms at the top of the column is measured at regular time intervals and compared to the initial total height of the fluid (H_t). H_s is visible in figure 5, where a picture of the samples at the end of the test is reported.

The primary metric derived is the Sedimentation Ratio, typically calculated as:

$$S_{\text{ratio}} = \left(\frac{H_s}{H_t}\right) * 100. \tag{2}$$

The principal advantages of this method are its simplicity and low cost, requiring no specialized equipment, however being largely qualitative. For the specific application case, this is significant, as the fluid inside the application is not moving while the vehicle is not operated, following the same test behaviour.

The results of the sedimentation percentage are reported in figure 6, where it is possible to see how, after 200 d, the percentage of separated fluid is different for whole the fluids, as it not only depends on the particle volume percentage, but also for the solvent used during the mixture and even by the surface treatment of the carbonyl iron particles. The most interesting behaviour is the one of fluid MRF1,

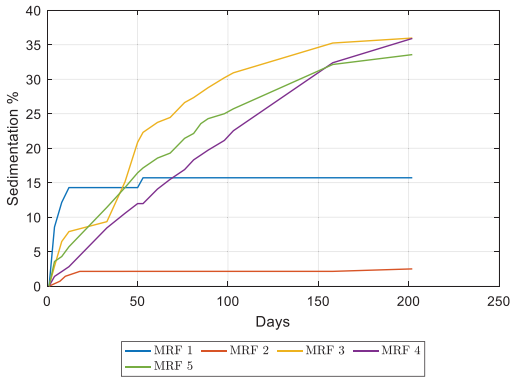

Figure 6. Sedimentation comparison—fluid separated percentage vs duration of the test (days).

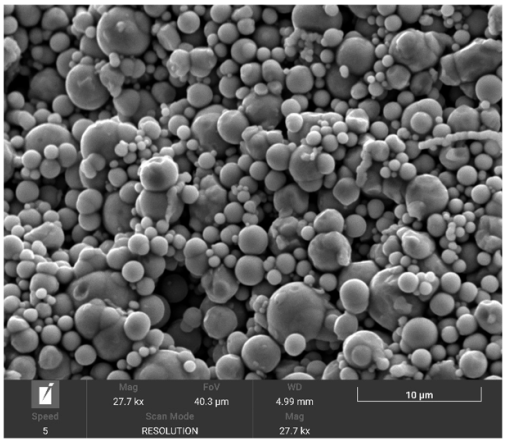

Figure 7. SEM characterization—example of an image of MRF 1 used for the distribution analysis.

capable of reaching stability in the fastest time, even if the separation percentage is equal to around 15%. MRF2 is the most stable, having just 2% of separated fluid at stability.

3.3. SEM characterization

After the first step of recovering pictures for each fluid as figure 7, reported for MRF 1, the distribution analysis has been performed.

Through the digital tools supported by the Leo Supra, it is possible to analyse the dimensions of each single particle, evaluating the average distribution of particle dimensions for each fluid.

As it is possible to see in figure 8, the particles diameter is expressed in μm and distributed into a histogram according to 0.5 μm classes. After the recognition of the different classes, it has been possible to obtain a Gaussian theoretical expression [20] reported in equation (3) as:

$$f(\chi) = \frac{1}{\sigma\sqrt{2\pi}} e^{-\frac{1}{2}\left(\frac{(\chi-\mu)}{\sigma^2}\right)} \tag{3}$$

where:

- $f(x)$ is the probability density at a point x.
- μ is the mean of the distribution, which defines its centre.
- σ is the standard deviation, which defines the spread or width of the distribution.

To analyse the SEM micrographs, the ImageJ software was utilized, allowing for the direct measurement of the metallic particles' cross-sectional areas after calibrating the pixel-to-μm ratio. As shown in the statistical distributions (figure 8), the highest-performing fluids exhibit a particle size range predominantly between 0.3 and 1.8 μm.

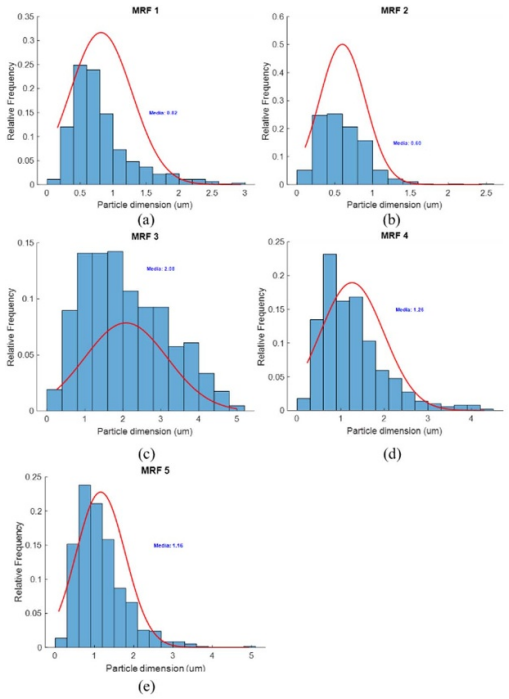

Figure 8. SEM analysis—particle dimension distribution for (a) MRF 1 (b) MRF 2 (c) MRF 3 (d) MRF 4 (e) MRF 5.

Table 4. SEM analysis—particle dimension distribution average.

Fluid type	Particle dimension average (μm)
MRF 1	0.82
MRF 2	0.60
MRF 3	2.04
MRF 4	1.26
MRF 5	1.16

It is critical to observe that for these specific fluids, the theoretical Gaussian distribution is truncated on the left tail, specifically below the 0.3 μm threshold. This truncation is not necessarily indicative of an absence of smaller particles but rather occurs because it reaches the resolution limit of the SEM instrument under the operating conditions used for this study. This morphological evidence strongly suggests the presence of a sub-300 nm metallic particle fraction.

Consequently, it is highly probable that these specific formulations employ a bidisperse composition, mixing micro- and nanoparticles, even if not explicitly disclosed by the manufacturer. The presence of this nanometric fraction fills the interstitial gaps between larger microparticles, reinforcing the magnetic chain structures. This clearly explains the enhanced peak shear stress performance of these fluids when compared to traditional, strictly micro-particle-based baseline fluids (e.g. the LORD 132 DG sample), which exhibited a strictly larger mean particle size of 2.27 μm, a significant fraction of 3–4 μm particles, and no evidence of left-tail truncation.

Computing the diameter average reported in table 4, allows to compare the fluid microscopic formulation for what concerns the solid part. In fact, according to multiple sources [21, 22], the impact of the particle shapes and dimensions is significant for the chains generation and, as a consequence, the shear stress action generated.

For this reason, the data obtained by the SEM analysis are pivotal for better understanding the rheological differences between one fluid and another.

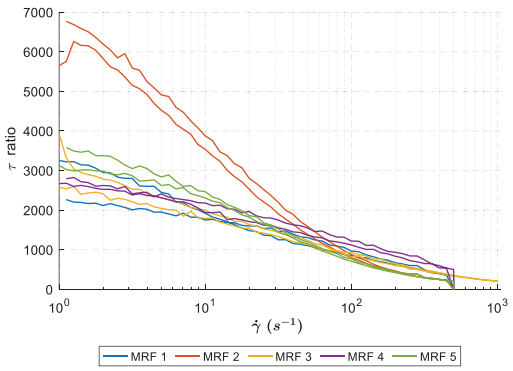

Figure 9. Rheological characterization—comparison of the on-state/off-state shear stress ratio as a function of the shear rate.

4. Discussion

The experimental results provide a rich dataset for a comparative analysis of the fluids' performance and for understanding the underlying structure-property relationships that govern their behaviour. This section synthesizes these findings to build a framework for application-specific fluid selection.

4.1. Analysis of the fluid behaviour comparison

The rheological analyses reported in this paper underline how the MRF 2 has the higher peak shear, so it manages to generate the higher amount of torque in a braking application. This effect could be explained by the higher volume percentage of particle in the fluid, as reported in table 2. The concentration, although is not the only parameter affecting the peak shear value, as it is possible to underline how MRF 5 generate the second highest peak shear stress, without being the second highest in concentration. An important aspect for determining the peak shear stress is also connected to the presence and distribution of nanoparticles mixed with microparticles. In fact, as described in multiple researches [23–25] the presence of nanoparticle is described as a way for reinforcing the metal particles chains under magnetization, allowing to filling the gap between a microparticle and another. The presence of nanoparticles in MRF 2 and MRF 5 is visible in figure 8, showing the distribution on smaller dimensions.

Peak shear stress is not the only critical aspect to be taken into the analysis, because for some applications, the shear stress in the off-state is particularly critical for defining the effective rolling resistance.

The most important consideration is regarding the need of defining a ratio between the shear stress during on-state versus the value at off-state varying the shear rate. This parameter is important to evaluate the fluid to be chosen while the application needs not only to maximize the braking torque, but also minimizing the rolling resistance action during off-state.

For this reason, the τ_{ratio} has been evaluated and plotted in figure 9.

It is possible to underline how the graph is characterized by the behaviour of MRF 2, that separates the analysis into two sections: up to a shear rate lower than 10^2 the ratio is around two times higher than the other fluids, defining how the solution is not only the one with the higher shear stress in the on-state, but also during the off-state is quite similar to the others. From 10^2 onwards, although, the MRF 2 ratio is quite similar to the others, while the better ratio is given by MRF 4. That means that, in case of an application that needs to be operative at high rotating speed predominantly, where there is an important operative time in off-state, MRF 4 should be the better solution. This effect could be described predominantly by the different oil base used, as its effect is predominantly visible during the off-state.

Regarding the sedimentation, it is possible to underline how the impact of the viscosity of the fluid is strictly interconnected with the stability of the mixture.

This physical relationship dictates that utilizing a carrier fluid with a higher base viscosity inherently restricts particle mobility and retards sedimentation, thereby significantly enhancing the long-term stability of the mixture [9]. However, an increase in the base oil's viscosity simultaneously elevates the fluid's macroscopic zero-field (off-state) viscosity [7]. In the context of automotive braking systems, this elevated off-state viscosity is highly detrimental. It directly translates to increased parasitic drag, elevated rolling resistance, and greater mechanical energy losses when the brake is disengaged.

Table 5. Optimal fluid for each application.

Category	Fluid type
Peak braking	MRF 2
High speed long off-state	MRF 4
Low speed long off-state	MRF 2
Low current	MRF 2

4.2. Fluid selection for different applications

This paragraph sums up the main cases to be taken into analysis for the use of the MRF into an automotive braking application. The scope of the analysis is to underline the optimal fluid between the five under test to be chosen according to the following operative cases:

1. Peak braking action
2. High speed with long off-state conditions
3. Low speed with long off-state conditions
4. Low current Application

For the first case the most critical curves to be taken into consideration are figures 2 and 3, for defining the peak braking torque available with the given fluid as a consequence.

For cases 2 and 3, it is critical to analyse results of figures 1 and 9, for better understand the off-state behaviour of each fluid.

For case 4, checking the figure 4 with the magneto-sweep is fundamental for analysing the higher shear to magnetic field point, in order to minimize the current to be used for supplying the electromagnets for the activation of the MRF.

In table 5 it is possible to summarize the better fluid between the ones tested for each category.

For applications where maximizing braking force is the sole priority, MRF 2 is the unequivocal choice due to its superior on-state shear stress and yield stress. For applications where the vehicle operates for long periods at high speeds with minimal braking, such as long-haul trucking, MRF 4 would be more advantageous due to its lower parasitic drag. For urban driving cycles with frequent low-speed braking and stops, MRF 2's high dynamic range at low shear rates makes it ideal.

Finally, it is essential to consider long-term stability as an overarching requirement for any automotive application. Phase separation can lead to unpredictable performance and catastrophic failure of the braking system. In this regard, MRF 2's exceptional stability (∼2% sedimentation) makes it the most robust and reliable choice overall. Even if another fluid offers a slight performance advantage in a niche operating condition, the risk associated with its lower stability may be unacceptable. Therefore, MRF 2 represents the safest engineering choice for a broad range of automotive braking applications.

5. Conclusion

This study successfully established and validated a comprehensive testing protocol for the systematic evaluation of MRFs tailored for automotive braking systems. The comparative analysis of five distinct fluids revealed significant performance trade-offs crucial for application-specific selection. Specifically, MRF 2 demonstrated superior performance in scenarios demanding maximum braking force, exhibiting the highest on-state shear stress. This was attributed to its high volume of solid content and a bimodal particle size distribution, including nanoparticles, which enhances chain formation under a magnetic field. Furthermore, MRF 2 showed the greatest stability, with minimal particle sedimentation over a 200 day period, a critical factor for vehicle longevity and reliability. Conversely, for applications involving high rotational speeds with prolonged off-state conditions, such as highway cruising, MRF 4 proved to be more advantageous. It presented the most favourable on-state to off-state shear stress ratio at high shear rates, minimizing parasitic drag and improving overall vehicle efficiency.

The characterization performed provides the necessary flow curves and material data to accurately model these fluids in CFD software, enabling more precise simulation of braking system performance. This work establishes a clear methodology for selecting the mosstabilityt appropriate MR fluid by bridging the gap between fundamental material properties and real-world performance metrics.

Future work should build upon these findings by addressing several key areas. Long-term durability and lifecycle testing is necessary to evaluate fluid degradation under extended thermal and mechanical cycling that simulates thousands of braking events, following the procedure already built in previous analyses [26]. Further improvements to fluid robustness could be achieved by investigating the influence of advanced additives on enhancing sedimentation stability and thermal range. Ultimately, the progression of this research involves integrating the most promising fluid (MRF 2) into a full-scale brake prototype for vehicle-level testing. This critical step will enable the validation of system performance, the refinement of control strategies, and a direct comparison against conventional friction braking systems under real-world driving conditions.

Acknowledgments

The research team aknowledges Guglielmo Peruzzi for his invaluable work in supporting the team in the definition of the testing plan. The results of this research are part of the activity funded by the Programma NODES-Nord Ovest Digitale E Sostenibile (Grant agreement Cod. n.ECS00000036) del finanziato dal MUR sui fondi M4C2–MISSIONE 4 COMPONENTE 2, 'Dalla ricerca all'impresa' INVESTIMENTO 1.5, avviso 'Ecosistemi dell'innovazione' nell'ambito del PNRR finanziato dall'Unione europea NextGenerationEU—Bando PoC Accademici a valere sui fondi CUPE13B22000020001–Spoke-2-'MATERIALIZED'.

Data availability statement

The data cannot be made publicly available upon publication because they contain commercially sensitive information. The data that support the findings of this study are available upon reasonable request from the authors.

Author contributions

Giovanni Imberti 0000-0003-4611-6802
Conceptualization (equal), Data curation (equal), Formal analysis (equal), Writing – original draft (equal)

Henrique de Carvalho Pinheiro 0000-0001-8116-336X
Investigation (equal), Methodology (equal), Writing – original draft (equal)

Massimiliana Carello
Funding acquisition (equal), Project administration (equal), Writing – review & editing (equal)

Lucia Tsantilis
Data curation (equal), Supervision (equal), Validation (equal)

Rajandrea Sethi
Resources (equal), Software (equal)

References

[1] Phulé P 2001 Magnetorheological (MR) fluids: principles and applications *Smart Mater. Bull.* **2001** 7–10
[2] Imberti G, Pinheiro H D C and Carello M, 2022 Design of an innovative zero-emissions braking system for vehicles *2022 Int. Conf. on Electrical, Computer, Communications and Mechatronics Engineering (ICECCME)* pp 1–6
[3] Pinheiro H D C, Imberti G and Carello M 2023.Pre-design and feasibility analysis of a magneto-rheological braking system for electric vehicles *SAE Technical Paper 2023–01–888* (SAE International) (https://doi.org/10.4271/2023-01-0888)
[4] Tempone G P, Carlo M D, Carello M, Pinheiro H D C and Imberti G 2025 A zero-emissions braking system: experimental setup, system characterization and model validation *SAE Technical Paper 2025–01–8250* (SAE International) (https://doi.org/10.4271/2025-01-8250)
[5] Imberti G, de Carvalho Pinheiro H and Carello M 2024 Impact of the braking system generated pollutants on the global vehicle emissions: a review *New Developments in Environmental Science and Engineering* ed X Chen (Springer) 11–19
[6] Rouabah S, Didouche F-Y, Khebli A, Aguib S and Chikh N 2025 The advancing understanding of magnetorheological fluids and elastomers: a comparative review analyzing mechanical and viscoelastic properties *Magnetochemistry* **11** 62
[7] Chauhan V, Kumar A and Radhey S 2024 Magnetorheological fluids: a comprehensive review *Manuf. Rev.* **11** 6

[8] Ashtiani M, Hashemabadi H and Ghaffari A 2014 A review on the magnetorheological fluid preparation and stabilization *J. Magn. Magn. Mater.* **374** 716–30
[9] Choi S-B 2022 Sedimentation stability of magnetorheological fluids: the state of the art and challenging issues *Micromachines* **13** 1904
[10] Park E J, Stoikov D, da Luz L F and Suleman A 2006 A performance evaluation of an automotive magnetorheological brake design with a sliding mode controller *Mechatronics* **16** 405–16
[11] Maurya C and Sarkar C 2024 Magnetorheological fluids: a comprehensive review of operational modes and performance under varied circumstances *Rheol. Acta* **63** 765–85
[12] Laun H M, Gabriel C and Kieburg C 2010 Twin gap magnetorheometer using ferromagnetic steel plates—performance and validation *J. Rheol.* **54** 327–54
[13] Del Gaudio C, Crognale V, Serino G, Galloni P, Audenino A, Ribatti D and Morbiducci U 2017 Natural polymeric microspheres for modulated drug delivery *Mater. Sci. Eng. C* **75** 408–17
[14] Paturi U M R, Kumar G and Vamshi V S 2020 Silver nanoparticle-based tween 80 green cutting fluid (AgNP-GCF) assisted MQL machining—an attempt towards eco-friendly machining *Clean. Eng. Technol.* **1** 100025
[15] Peruzzi G, Imberti G, de Carvalho Pinheiro H, Tsantilis L, Sethi R and Santagata E 2025 Rheological characterization of magnetorheological fluids for brake applications: an experimental procedure *Fluids* **10** 2
[16] Jonkkari I, Kostamo E, Kostamo J, Syrjala S and Pietola M 2012 Effect of the plate surface characteristics and gap height on yield stresses of a magnetorheological fluid *Smart Mater. Struct.* **21** 075030
[17] Ma R and Wereley N M 2023 Sedimentation of magnetorheological fluids measured using an automated vertical axis inductance monitoring system *AIP Adv.* **13** 035016
[18] Kanda M, Kaide A, Saeki T and Tochigi H 2021 Preparation and rheology of magnetorheological fluid using six kinds of fumed silica as stabilizing additives *MATEC Web Conf.* **333** 02006
[19] Roupec J, Berka P, Mazůrek I, Strecker Z, Kubík M, Macháček O and Andani M T 2017 A novel method for measurement of MR fluid sedimentation and its experimental verification *Smart Mater. Struct.* **26** 107001
[20] Chen S 2024 The Gaussian distribution: derivation method and its applications in selected examples *Theor. Nat. Sci.* **38** 196–202
[21] Kim H Y, Kwon S H and Choi H J 2017 Magnetorheology of snowman-like anisotropic microparticle added carbonyl iron suspension *IEEE Trans. Magn.* **53** 1–4
[22] Huang J and Yang Y 2013 Micro-chain model of magnetorheological fluids between two parallel disks *The 8th Annual IEEE Int. Conf. on Nano/Micro Engineered and Molecular Systems* pp 1285–8
[23] Xu L and Zhou G 2024 Enhancement of magnetorheological fluids with size and morphology—optimized fe3o4 nanoparticles: impacts on rheological properties and stability *Materials* **17** 12
[24] Song K and Park B-J 2009 Effect of magnetic nanoparticle additive on characteristics of magnetorheological fluid *IEEE Trans. Magn.* **45** 4045–8
[25] Kormann C, Laun H M and Richter H J 1996 Mr fluids with nano-sized magnetic particles *Int. J. Mod Phys B.* **10** 3167–72
[26] Imberti G, de Carvalho Pinheiro H, De Carlo M, Peruzzi G and Carello M 2025 Durability analysis of a magneto-rheological fluid for automotive braking system *Designs* **9** 74